Research Article

Reducing Activation Energy in Novolac Resins through Bio-Oil Integration: A Sustainable Approach

Archana Bansode[†,‡], Iris Beatriz Vega Erramuspe[*,§], Lorena Alexandra Portilla Villarreal[§], Braden Hahn[‡], Brian K. Via[§], Allan David[‡], Nicole Labbé[¶], Maria L Auad[*,†,‡]

Abstract

This study presents the development of a bio-oil-enhanced curing system for novolac phenol-formaldehyde (PF) resins, aimed at advancing both the environmental sustainability and efficiency of these materials. By partially substituting phenol with bio-oil derived from the fast pyrolysis of pinewood biomass, we engineered a bio-based novolac resin with significantly improved curing characteristics. The introduction of bio-oil into the resin formulation led to a marked reduction in the curing temperature by approximately 20°C, a change driven by the additional reactive functional groups present in the bio-oil. These groups enhance the crosslinking potential of the resin, facilitating an earlier onset of curing reactions and reducing the overall activation energy required for the process.

The study employed dynamic differential scanning calorimetry (DSC) to assess the curing behavior of both conventional and bio-oil-enhanced resins. While the autocatalytic model demonstrated a strong fit for the conventional novolac resin and HMTA mixture, the Kamal model was found to be more appropriate for describing the curing dynamics of the bio-oil-based novolac resin. The Kamal model's effectiveness is attributed to its ability to capture the complex curing mechanism of the bio-based system, which involves an initial autocatalytic stage followed by a reaction governed by nth-order kinetics. This dual-stage mechanism reflects the unique influence of bio-oil on the resin's crosslinking behavior, providing a more accurate representation of the curing process. These findings highlight the potential of bio-oil as a valuable component in novolac PF resins, offering a pathway to more energy-efficient and sustainable materials.

Keywords: Bio-oil; Novolac Resin; Differential Scanning Calorimetry; Curing Reaction Kinetics; Model-Fitting; Building Design

Introduction

Novolac-type phenol-formaldehyde (NPF) resins are widely utilized in various industrial applications due to their exceptional mechanical properties, thermal stability, and chemical resistance.[1] These attributes are essential for meeting the stringent performance requirements in sectors such as automotive, construction, and electronics.[2] NPF resins are produced through an acid-catalyzed condensation polymerization reaction with a higher proportion of phenol reactant (P/F molar ratio 1:0.8), resulting in either linear or partially cross-linked structures interconnected by methylene bridges. The curing process involves the addition of a hardener, commonly hexamethylenetetramine (HMTA), which facilitates the formation of a three-dimensional network

polymer structure at elevated temperatures.3 The chemical interaction between NPF and HMTA progresses through two distinct stages of cross-linking.4 In the second stage, the intermediates undergo decomposition and initiate a reaction, resulting in the formation of methylene linkages between phenolic rings to extend the polymer chains further.5 However, synthesizing NPF resins still relies on nonrenewable resources, which are associated with the rapid depletion of fossil fuels and increasing concerns for the environment and individual's health.6 Therefore, substantial research is being conducted to investigate alternative sources, such as sustainable biomass, as substitutes for conventional petroleum-based feedstocks. Thermochemically derived materials are considered advantageous sources for bio-based monomers, including phenolic compounds, as they can be obtained during the thermochemical conversion of biomass. These derivatives can serve as an alternative reagent during polymer resin synthesis.,7–9

Once phenol in phenol-formaldehyde resins is partially replaced with bio-based materials, it is crucial to evaluate the properties of these modified resins. One critical property is the curing behavior, which directly influences the performance and applicability of the resin in industrial applications. Curing kinetics studies provide insights into the thermal stability, mechanical strength, and overall durability of the resin.10 Understanding the curing behavior of bio-based NPF resins is essential to ensure they meet or exceed the performance of traditional petroleum-based resins.

Recent advancements in the understanding of the curing kinetics of phenol-formaldehyde resins have been achieved through techniques such as Differential Scanning Calorimetry (DSC) and Thermogravimetric Analysis (TGA). For instance, studies utilizing DSC to investigate the curing behavior of phenol-formaldehyde resin-impregnated paper have provided critical insights into the resin's thermal properties and curing dynamics.10 Research on the impact of various accelerators, such as magnesium hydrate and methylolureas, has shown that these additives can significantly expedite the curing process and improve the resins' thermal stability.11 Moreover, the interaction between phenol-formaldehyde resins and wood substrates can alter the activation energy required for curing, affecting the overall efficiency of the process. Studies employing isoconversional methods, such as the Kissinger and Flynn-Wall-Ozawa techniques, have modeled these interactions to better understand the kinetic parameters and activation energy involved.12,13 Incorporating bio-based materials into phenol-formaldehyde resins has shown promising results. For example, Wuzella et al. (2020) investigated the isoconversional cure kinetics of a novel thermosetting resin based on linseed oil, finding that the incorporation of bio-based components could effectively modify the thermal curing behavior of the resin.14 Similarly, Zolghadr et al. (2019) explored the modification

of epoxy resins with bio-based furan derivatives, using DSC and TGA to reveal significant enhancements in curing kinetics and mechanical properties.15 Ferdosian et al. (2016) examined the curing kinetics and mechanical properties of bio-based epoxy composites comprising lignin-based epoxy resins, demonstrating that lignin-based resins exhibited comparable performance to conventional resins while offering environmental benefits.16 The incorporation of Kraft lignin to partially replace phenol has also shown promising results in reducing the curing temperature and improving the thermal stability of the resins, as demonstrated by Ray and Xu (2017).17 Cui et al. (2017) synthesized bio-oil phenol-formaldehyde (BPF) resin using bio-oil from the fast pyrolysis of renewable biomass. The study showed that incorporating bio-oil improved the crosslinking degree and thermal properties of the PF resin. The DSC and TGA analyses indicated that even at a 20% substitution level, the bio-oil had a positive impact on the resin's curing behavior.18 Another study by Song et al. (2021) focused on bio-based phenol-formaldehyde adhesives derived from demethylated wheat straw alkali lignin, showing that the modified resins had a faster curing rate and higher bonding strength compared to conventional PF resins.19

Differential scanning calorimetry (DSC) stands out as a precise method for studying the curing reactions of thermosetting resins, evaluating heat flow over temperature and time to estimate kinetic parameters. Isothermal and non-isothermal thermal kinetic analysis methods are extensively used, with non-isothermal processes offering significant advantages. The model-free (isoconversional) technique and the model-fitting approach are primarily employed to fit experimental data from DSC curves to estimate activation energy and kinetic parameters. For instance, Zhang et al. explored the curing characteristics of novolac phenol-formaldehyde using both model-fitting and isoconversion kinetic methodologies, employing a segmented kinetic model that effectively describes the curing kinetics of novolac.20 Despite thorough investigations on the curing reaction of phenol-formaldehyde compounds, no prior scientific inquiry has specifically addressed the kinetics of the curing process for biobased phenol-formaldehyde resin synthesized by partially replacing phenol with bio-oil from the rapid pyrolysis of pinewood.

The primary focus of this study is to conduct a comprehensive investigation into the curing behavior of bio-based novolac phenol-formaldehyde (BNPF) resins. Utilizing the DSC method, this research aims to thoroughly examine the curing process of the resin from initiation to completion. DSC data will be analyzed to determine a detailed array of curing kinetic attributes, using dynamic heating profiles for curing analysis. Both isoconversional and model-fitting methodologies will be employed to derive insights that are pivotal for understanding the curing behavior of BNPF. This

knowledge will guide the optimization of resin manufacturing processes, leading to the production of high-performance materials derived from sustainable resources.

Experimental Section

Materials

Phenol in its solid state (99% purity), a formalin solution (containing 37% formaldehyde in water), hexamethylenetetramine (HMTA, purity exceeding 99%), and acetone (with a purity of 99.5%) were sourced from VWR International. Anhydrous oxalic acid (with a purity of 98.0%) was purchased from Spectrum Chemical Mfg. Corp. Bio-oil, which was prepared using previously established protocols,21 was provided by the Center for Renewable Carbon Laboratory at the University of Tennessee. Detailed information on the purity of all compounds can be found in Table S1 in the supporting information section.

Synthesis of Novolac PF Resin and Bio-Based Novolac PF Resin

Novolac phenol-formaldehyde (NPF) and bio-based novolac phenol-formaldehyde (BNPF) were developed through the reaction of phenol with formaldehyde, following procedures outlined in a previously published article.8 In brief, phenol (1 mol, 94 g) and oxalic acid (0.05 mol, 4.70 g) were added to a 500 mL round-bottom flask, which was equipped with four necks, including a condenser, a dropping funnel, and a mechanical stirrer. 37% formalin solution (0.8 mol of formaldehyde, 64.87 g) was slowly added dropwise into the mixture, which had been heated to 90°C. The reaction product was washed with distilled water and subsequently dried in a vacuum oven after allowing the reaction to proceed at 90°C for a total duration of 3 hours. The biobased novolac PF was prepared with the same procedure by partially replacing (50% w/w) phenol with bio-oil. The reaction mechanism of bio-based novolac resin is presented in Figure S1. The characterization of the synthesized resin was reported in our previous journal8 and the corresponding FTIR and 1H-NMR results added in the supporting information as Figure S2 and Figure S3, respectively.

Thermal Analysis

The investigation into the curing reaction of NPF/HMTA and BNPF/HEXA was conducted utilizing a differential scanning calorimeter, specifically the DSC TA-Q2000 (Thermal Analysis Instruments, DE, USA). This analysis took place in a controlled nitrogen environment with a gas flow maintained at 50 mL/min. Prior to conducting any sample measurement, the DSC instrument underwent calibration using the standard of pure indium. The samples, NPF/HMTA and BNPF/HMTA were prepared with HMTA to resin weight ratio of 15% and ground manually with mortar and pestle. For each measurement, the sample (3.0 – 5.0 mg) was placed in the aluminum standard pan and capped with an aluminum cover.

The DSC non-isothermal technique investigated the curing behavior of both NPF/HMTA and BNPF/HMTA resins. Initially, the thermal data were acquired by incrementally heating the samples from 25°C to 250°C at different heating rates of (5, 10, 15, and 25°C/min). After the curing reaction concluded, the samples were cooled to 25°C at respective cooling rates of 5, 10, 15, and 25°C/min. Next, a non-isothermal curing experiment was conducted to assess the reaction's residual heat, employing the respective heating rates. Figure 1a illustrates the curing reactions of NPF/HMTA resins, while Figure 1b depicts those of BNPF/HMTA.

Origin Pro 2019 software (Origin Lab Corporation, USA) and MATLAB R2022a (version 9.0) were used to analyze thermal curing data.

Fundamental Theory of Curing Kinetics

Curing reaction kinetics are conducted to illustrate the correlation between reaction rates and various experimental parameters. The thermal data acquired through non-isothermal DSC technique for NPF/HMTA and BNPF/HMTA resins, across various heating rates, were utilized for the determination of kinetic parameters.

The degree of curing (α), representing the conversion of the curing reaction, correlates directly with the exothermic heat released throughout the curing process.22,23 The degree of curing (α) can be expressed from Eq (1)

$$\alpha(T) = \frac{\Delta H_T}{\Delta H_{total}} \tag{1}$$

where, ΔH_T represents the heat of reaction at a specific temperature, T, and ΔH_{total} represents the overall heat of the reaction, which is calculated by integrating the area under the exothermic curve. The curing reaction was considered complete when the non-isothermal exothermic peak of the resins reached a plateau at the baseline.

The rate of the kinetic process is deemed to be linearly related to the recorded heat flow and can be determined by Eq (2).

$$\frac{d\alpha}{dt} = \frac{\left(\frac{dH}{dt}\right)}{\Delta H_{total}} \tag{2}$$

where, $d\alpha/dt$ represents the rate of the curing kinetic reaction, dH/dt is heat flow observed during the kinetic process. During consistent heating rate scans, $d\alpha/dt$ can be represented as $d\alpha/dt = \beta\, d\alpha/dT$ at constant where β denotes the rate of heating (K min-1).

The phenomenological curing kinetic model analysis is parametrized into two main functions27 according to the following Eq (3)[24]

$$\frac{d\alpha}{dt} = k(T)f(\alpha) \tag{3}$$

where, k(T) signifies temperature-dependent kinetic rate
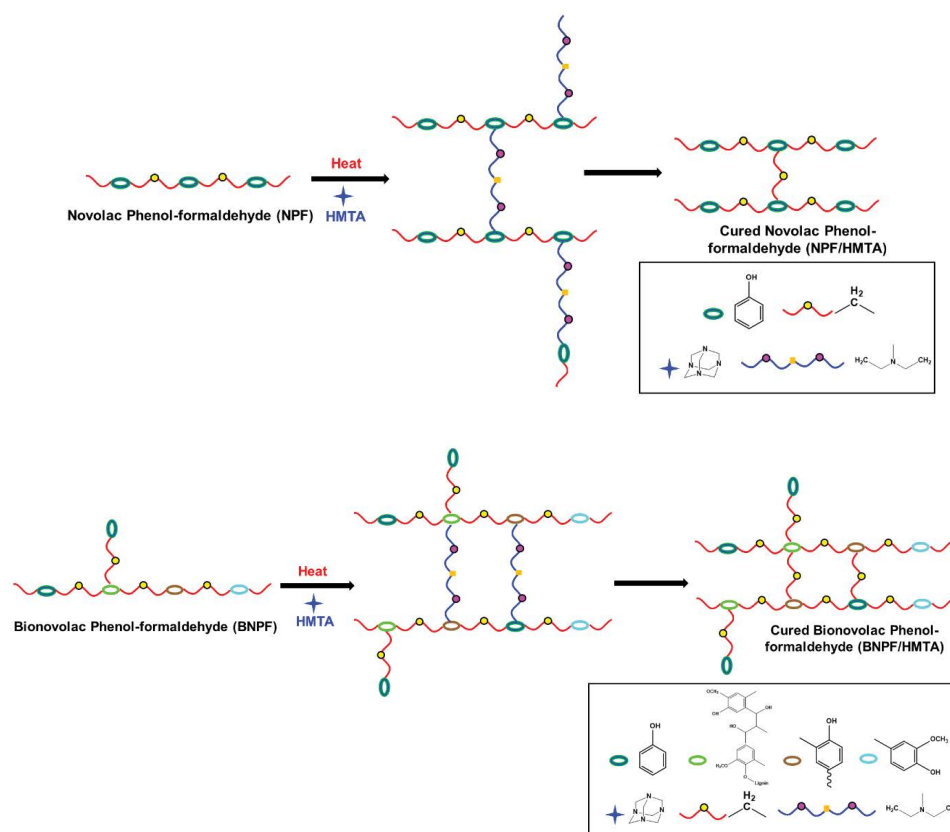
Figure 1: The process of curing (a) novolac phenol-formaldehyde resin with HMTA (NPF/HMTA) and (b) bionovolac phenol-formaldehyde resin with HMTA (BNPF/HMTA).

constant and f(α) is the function representing the conversion of curing.25 The function k(T) can be expressed through Arrhenius relationship as shown by Eq (4)[24]

$$k(T) = A \exp\left(-\frac{E}{RT}\right) \quad (4)$$

where, A represents Arrhenius frequency factor or pre-exponential factor (s-1), E is the activation energy (J mol-1), R is the universal gas constant (8.314 J mol-1 K-1), and T is the absolute temperature (K) of the sample. Combining Eq (3) and Eq (4) yields kinetic Eq (5)

$$\frac{d\alpha}{dt} = A \exp\left(-\frac{E}{RT}\right) f(\alpha) \quad (5)$$

Curing kinetic reactions are often analyzed by two primary methodologies, i.e., model-fitting kinetic technique and model-free Isoconversional kinetic methods. In the model-based approach, kinetic model is utilized to fit the experimental data to estimate the kinetic characteristics.26 Alternatively, the isoconversional kinetic method obeys isoconversional principle.26,27

Model-Free Isoconversional Method

The model-free is a valuable approach to determining the mechanism of curing, and the basic assumption of this method is that the rate of reaction is solely dependent on temperature, without being influenced by the degree of curing, as expressed by Eq (6).[26–28]

$$\left[\frac{\partial \ln(d\alpha/dt)}{\partial T^{-1}}\right] = -\frac{E}{R} \quad (6)$$

The most commonly used methods include Friedman,29 Flynn-Wall-Ozawa (FWO),30,31 Kissinger-Akahira-Sunnose (KAS),32 and Vyazovkin.26,33,34 These model-free isoconversional methods are used to calculate the re-activation energy (E) without assuming any specific expression of the reaction model.

Model-Fitting Method

The mechanism of curing reaction of resin that is related to the curing kinetic reaction modelf(α), can be divided into three kinetic models: nth-order model, autocatalytic model, and Kamal-Sourour model.20,25,35 These models can be characterized by Eq (7), Eq (8), and Eq (9), respectively.

nth-order kinetics model can be represented as

$$\frac{d\alpha}{dt} = A \exp\left(-\frac{E}{RT}\right) (1-\alpha)^n \quad (7)$$

The autocatalytic kinetic model can be represented as

$$\frac{d\alpha}{dt} = A \exp\left(-\frac{E}{RT}\right) (1-\alpha)^n \alpha^m \quad (8)$$

The Kamal kinetic model can be expressed as

$$\frac{d\alpha}{dt} = k_1 (1-\alpha)^n + k_2 (1-\alpha)^n \alpha^m \qquad (9)$$

where m and n are the reaction orders, $k_1 = A_1 \exp(-E_1/RT)$ and $k_2 = A_2 \exp(-E_2/RT)$ are the kinetic constants. The parameters A1 and A2 stand for the pre-exponential parameters, while E1 and E2 represent the activation energies.

Results and Discussion

Non-Isothermal DSC Analysis of NPF/HMTA and BNPF/HMTA Resins

Isothermal and non-isothermal DSC measurements were conducted to quantify the heat of the reaction and understand the curing behavior of developed NPF/HMTA and BNPF/HMTA resins. The isothermal approach yielded higher testing errors, similar to those previously reported for other systems.36 Therefore, the non-isothermal DSC technique was adopted.

The non-isothermal DSC profiles of the NPF/HMTA and BNPF/HMTA resins using various heating rates of 5, 10, 15, and 25°C/min are depicted in Figure 2a and Figure 2b, respectively. Each of the thermograms displays distinct exothermic signals, indicative of the intricate chemical transformations occurring during the curing processes of the NPF/HMTA and BNPF/HMTA resins. The peak temperature (Tp), derived from these pronounced exothermic signals, has been systematically compiled and is detailed in Table 1. As the heating rates (β) were incremented from 5 to 20°C/min, it was observed that all the exothermic peaks associated with the curing processes exhibited a discernible shift toward higher temperatures. This phenomenon was also reflected in the alteration of characteristic peak temperatures. The aforementioned increments can be elucidated as follows: the observed rise in temperature with increasing heating rates stems from the greater heat flux generated during the process. Consequently, this elevated heat flux leads to intensified thermal gradients between the reaction center and the surrounding environment. This phenomenon can be attributed to the inherent thermal inertia of the system, wherein the rate of temperature change is influenced by the thermal properties of the materials involved.36–38 The phenomenon of the exothermic peak temperature shifting towards higher temperature regimes is typically attributed to compensatory mechanisms. In response to increased heating rates, the system undergoes adjustments to accommodate the higher thermal energy input, resulting in a shift of the exothermic peak temperature.39 In the case of the DSC curves of BNPF/HMTA resin, the presence of two distinct exothermic peaks suggests the occurrence of multiple consecutive or concurrent reactions within the resin matrix. The first broad exotherm is attributed to the primary curing reaction, reflecting the onset of cross-linking processes within the resin matrix. Concurrently, a smaller exothermic peak observed at higher temperatures

is suggestive of secondary reactions occurring during the heating process. These secondary reactions likely involve interactions between other chemical functionalities and the intermediates produced by the HMTA. Despite the presence of these secondary reactions, the associated exothermic peak is relatively minor in magnitude and was therefore disregarded in the current investigation. Consequently, only the exothermic peak corresponding to the primary curing reaction was considered for kinetic analysis. The presence of bio-oil introduced additional reactive functional groups into the resin matrix, which enhanced the crosslinking potential. This was evidenced by the observed reduction in the curing temperature by approximately 20°C compared to the conventional NPF/HMTA resin. The incorporation of bio-oil led to a modified crosslinking density within the resin, which facilitated the earlier onset of crosslinking reactions. This change in the crosslinking dynamics is attributed to the chemical composition of bio-oil, which not only provides additional phenolic structures but also introduces various oxygenated compounds that are more reactive under curing conditions. These compounds are likely to interact with the HMTA curing agent more readily, lowering the activation energy required for the curing process.
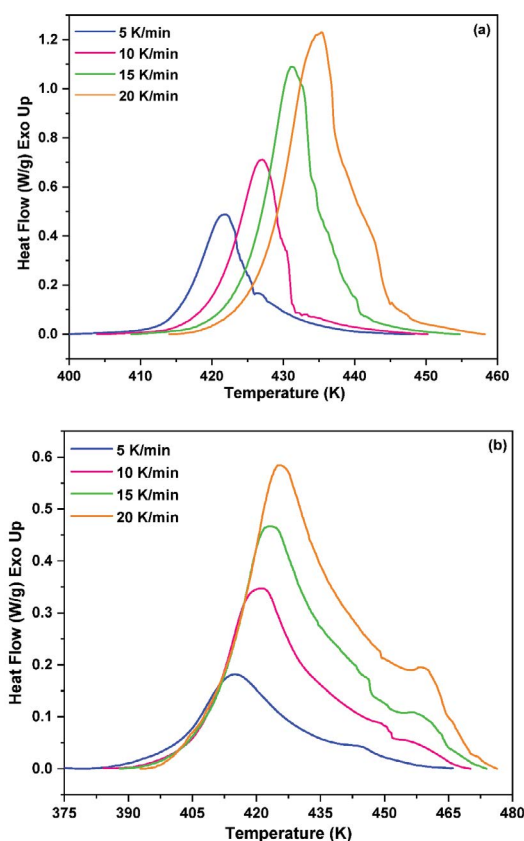
Figure 2: The differential scanning calorimetry (DSC) thermograms obtained from non-isothermal scanning depict the thermal curing reactions of (a) NPF/HMTA resin and (b) BNPF/HMTA resin. These thermograms were acquired at various heating rates, including 5, 10, 15, and 20 K/min.

Citation: Archana Bansode, Iris Beatriz Vega Erramuspe, Lorena Alexandra Portilla Villarreal, Braden Hahn, Brian K. Via, Allan David, Nicole Labbé, Maria L Auad. Reducing Activation Energy in Novolac Resins through Bio-Oil Integration: A Sustainable Approach. Journal of Radiology and Clinical Imaging 8 (2025): 88-99.

Table 1: Characteristic Parameters of the curing reactions of NPF/HMTA and BNPF/HMTA

Heating rate (β)	NPF/HMTA resin	BNPF/HMTA resin
(K/min)	T_P (K)	T_P (K)
5	421.81	415.11
10	426.97	420.9
15	431.21	423.1
20	435.44	425.72

NPF: novolac phenol-formaldehyde resin. BNPF: Bio-based novolac phenol-formaldehyde resin. HMTA: hexamethyl tetraamine (hardener). Tp: Curing peak temperature. HMTA: hexamethyl tetraamine (hardener). Tp, Curing peak temperature.

Model-Fitting Method

The objective of the model-fitting kinetic analysis concerning NPF/HMTA and BNPF/HMTA resins was to ascertain the four kinetic parameters (A, E, n, m), as delineated in equations 7, 8, and 9, pertaining to the curing system based on an appropriate reaction model. To rigorously scrutinize the kinetic model, the activation energy (E) is meticulously computed by substituting the expression for the heating rate (β = dT/dt) into Eq. (6). The logarithmic transformation of this expression, as outlined in Eq. (10), enables a profound investigation into the interplay between the peak temperature (Tp) and the heating rate (β). Under the assumption of an isofractional peak temperature (Tp = Constant), the activation energy E is determined by a linear regression analysis of ln(βdα/dTp) against 1/Tp across various heating rates (5, 10, 15 and 25 K/min) as reported in Eq (10) and shown in Figure 3.

$$E = \frac{Rd\left[-\ln(\beta d\alpha/dT_p)\right]}{d(1/T_p)} \qquad (10)$$
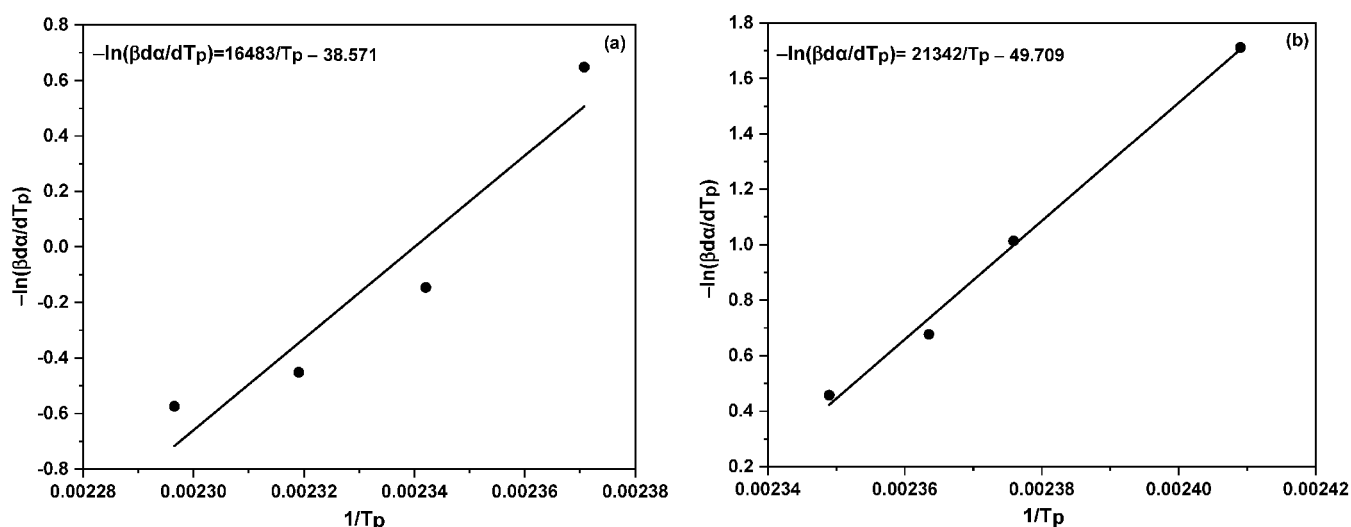
Utilizing the activation energy and with meticulous consideration for selecting the suitable kinetic model, the determination of the reaction order (n or m) and the frequency factor (A) is undertaken. This process involves intricate mathematical calculations and detailed analysis to precisely quantify the kinetics of the reaction.

For nth-order model, by taking the logarithmic form of Eq (7), which is reported in the theory section, and expressing it in Eq (11)

$$\ln\left(\frac{d\alpha}{dt}\right) + \frac{E}{RT} = n \ln(1-\alpha) + \ln A \qquad (11)$$

Through the application of the linear regression technique to Eq (11), the values for n and A are derived from the slope, representing n, and the intercept, denoted by ln A, respectively. Regarding the autocatalytic model, upon performing a logarithmic transformation of Eq (8) as outlined in the theory section, it results in the derivation of Eq (12).

$$\ln\left(\frac{d\alpha}{dt}\right) + \frac{E}{RT} = n \ln(1-\alpha) + m \ln \alpha + \ln A \qquad (12)$$

To ascertain the values of A, n, and m, a rigorous multilinear regression technique is employed on Eq (12). Specifically, within the framework of the autocatalytic model, the determination of the overall reaction order (m + n) can be approached with or without constraints. This involves considering the sum of the individual reaction orders, m and n, which collectively represent the overall reaction order. The choice between utilizing constraints (m + n = 2) or not imposes specific conditions on the overall reaction order determination.

In the context of the Kamal model, a comprehensive approach is employed to estimate the kinetic parameters and reaction orders (n and m) through the utilization of a nonlinear regression method. This intricate technique involves fitting the model's equation to experimental data,

Figure 3: Activation energy determination of the (a) NPF/HMTA resin and (b) BNPF/HMTA resin systems.

Citation: Archana Bansode, Iris Beatriz Vega Erramuspe, Lorena Alexandra Portilla Villarreal, Braden Hahn, Brian K. Via, Allan David, Nicole Labbé, Maria L Auad. Reducing Activation Energy in Novolac Resins through Bio-Oil Integration: A Sustainable Approach. Journal of Radiology and Clinical Imaging 8 (2025): 88-99.

allowing for the meticulous determination of the model's parameters. Furthermore, in the case of the Kamal model, a variety of conditions were meticulously applied to scrutinize the kinetic constants, denoted as k1 and k2 (E1 = E2 & m + n = 2, E1 = E2 & m + n ≠ 2, E1 ≠ E2 & m + n = 2 and E1 ≠ E2 & m + n ≠ 2). The computational analysis and evaluation of these intricate parameters were conducted utilizing the MATLAB R2022a software (version 9.0), renowned for its robust capabilities in numerical computation and analysis.

Following the meticulous determination of kinetic parameters at various heating rates for the nth-order model (comprising E, A, and n), autocatalytic model (comprising E, A, m, and n), and Kamal model (including E1, E2, A1, A2, m, and n), the subsequent procedural stage involves the precise fitting of experimental data utilizing the corresponding model alongside the ascertained kinetic parameters. This fitting endeavor is undertaken to acquire crucial metrics such as the degree of curing (α) and reaction rate (dα/dt) at each specific temperature. The outcomes of this comprehensive process, depicting the results of the curing kinetic model obtained through the fitting models, are systematically elucidated and summarized in Table 2 for analytical reference and interpretation.

Table 2: The outcomes derived from the analysis of curing kinetics through both the autocatalytic model and the Kamal model.

Resins	E_a (KJ/mol)	A (min^{-1})	n	m
NPF/HMTA	137	1.982×10^{17}	1.2342	0.7658
BNPF/HMTA	1.195 E1=E2	A1=1.734 ×10^{-8} A2=3.038	1.1948	0.8051

Upon meticulous observation and analysis of the extent of conversion (α) plots concerning both NPF/HMTA and BNPF/HMTA, as depicted respectively in Figure 4 and Figure 6, a discernible sigmoidal profile prominently emerges. This distinctive profile manifests as a gradual ascent in α during the initial and final stages of the curing process, juxtaposed with a notably swift acceleration observed at the intermediate phase. Furthermore, it is noteworthy to highlight that the elevation of heating rates induces a discernible displacement of these conversion (α) curves towards higher temperature regimes. This observed phenomenon not only underscores the intricate dynamics of the curing process but also underscores the robustness of the experimental findings. Additionally, the consistency of these observations with similar studies further accentuates the reliability and validity of the experimental data, thereby augmenting our understanding of the underlying kinetics governing the curing process.36

Based on the comprehensive analysis of model fitting outcomes about NPF/HMTA resin, it becomes evident that the autocatalytic model offers a notably favorable fit for the experimental data, as meticulously depicted in both Figure 4 and Figure 5. This favorable agreement can be

attributed to the intrinsic nature of the autocatalytic curing mechanism, which exerts significant control over the entire curing reaction process of NPF/HMTA resin. The underlying mechanism involves the generation of intermediate products throughout the curing process, which in turn catalyzes the reaction, particularly notable due to their involvement in reactions characterized by a higher order of reaction (n). Remarkably, the reaction rate attains its zenith at the midpoint of the reaction stage, underscoring the pivotal role played by these intermediates in catalyzing the curing process. Furthermore, an intriguing observation emerges from the analysis, wherein a smaller reaction order (m) is discerned, indicative of a scenario where the curing rate of the reaction experiences a decline. This nuanced insight into the kinetics of the curing process not only enriches our understanding but also resonates with findings documented in published works, further corroborating the robustness and reliability of our experimental results. This alignment with existing literature, as evidenced by the citation of relevant works20,40,41, underscores the consistency and validity of our findings within the broader scientific discourse.

As delineated in both Figure 6 and Figure 7, the Kamal model emerges as a highly adept tool for predicting and monitoring the intricate nuances of the curing mechanism governing the BNPF/HMTA resin. This assertion is substantiated by the remarkable alignment observed between the kinetic model predictions and the experimental data, underscoring the model's robust predictability.

The Kamal model, a composite framework amalgamating aspects of both the nth-order and autocatalytic models, offers a nuanced depiction of the curing process dynamics. During the initial phase of the curing process, wherein the curing agent undergoes decomposition, giving rise to intermediates that subsequently engage in reaction with the novolac resin, the mechanism is primarily influenced by autocatalytic reactions. However, as the curing process progresses into its later stages, the influence of the nth-order reaction mechanism becomes increasingly pronounced. This transition is attributable to the diminishing availability of free phenol and phenolic hydroxyl groups, which govern the reaction rate and contribute to its gradual decline.

The curing mechanism, as captured by the Kamal model for BNPF/HMTA resin, reflects this complexity. Initially, the autocatalytic mechanism dominates, driven by the rapid reaction of these oxygenated compounds with the HMTA, resulting in a quick build-up of crosslinked structures. As the reaction progresses, the nth-order kinetics become more pronounced, controlling the later stages of curing where the availability of reactive sites decreases. This dual mechanism, accurately modeled by the Kamal framework, underscores the role of bio-oil in altering the curing pathway, leading to a more energy-efficient process. The introduction of bio-oil not only affects the thermal behavior of the resin but also

has broader implications for the material properties, such as improved flexibility and toughness, which are essential for various industrial applications. The reduction in curing temperature not only offers environmental benefits by reducing energy consumption but also enhances production safety by lowering the operational temperatures required during resin processing.
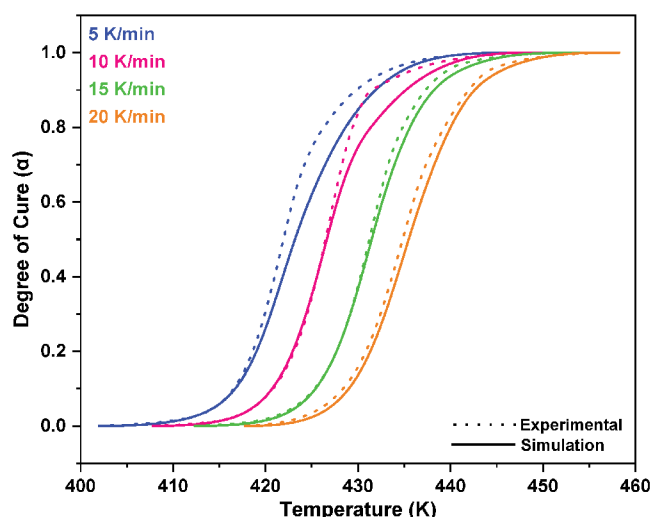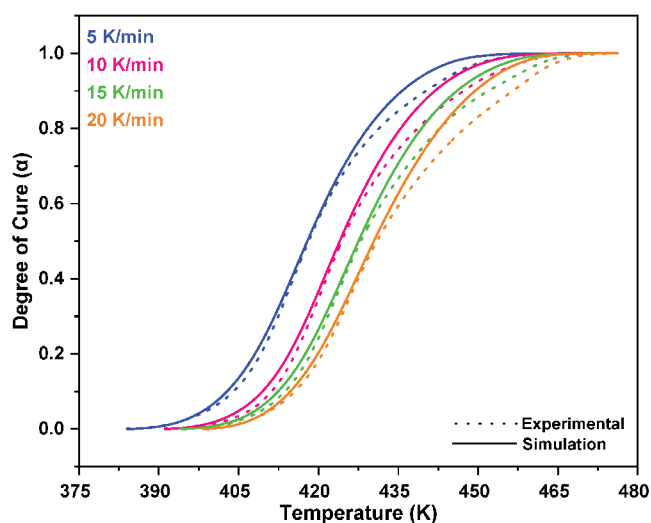

Figure 4: Graphical depiction illustrating the conversion (α) as a function of temperature. This plot provides a comparative analysis between the experimental data and the simulated results for NPF/HMTA resin at varying heating rate conditions.
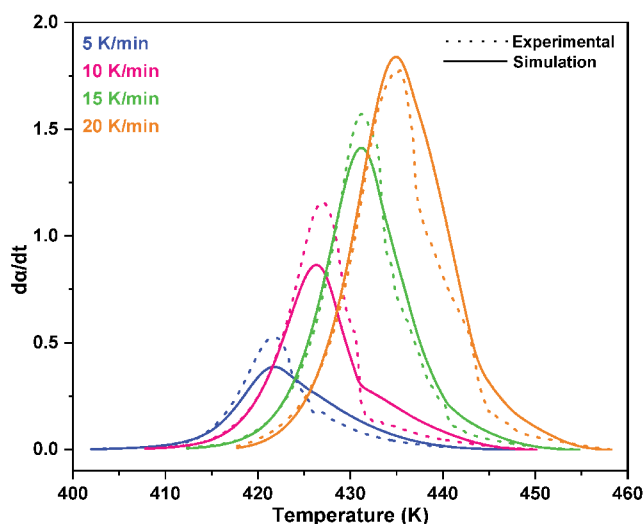
Figure 5: Graphical representation depicting the reaction rate (dα/dt) as a function of temperature, showcasing a comparative analysis between the experimental data and the simulated results for NPF/HMTA resin across various heating rates.

Conclusion

The study systematically examined the curing behavior of novolac-type phenol-formaldehyde (PF) resins, comparing conventional NPF/HMTA resins with bio-based novolac

Figure 6: Graphical depiction illustrating the conversion (α) as a function of temperature. This plot provides a comparative analysis between the experimental data and the simulated results for BNPF/HMTA resin at varying heating rate conditions.
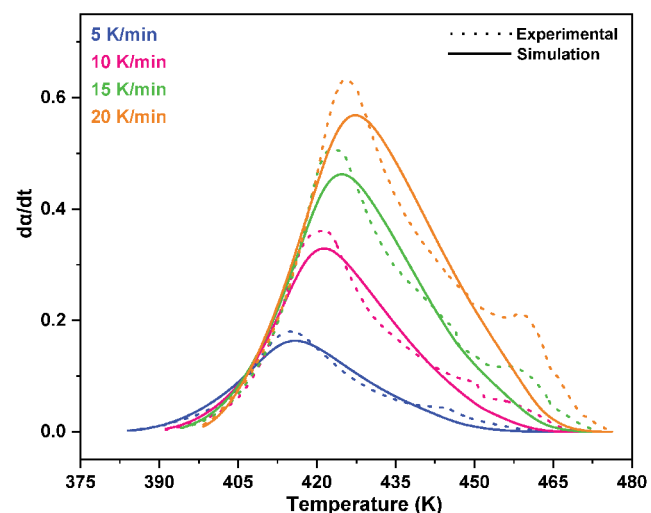

Figure 7: Graphical representation depicting the reaction rate (dα/dt) as a function of temperature, showcasing a comparative analysis between the experimental data and the simulated results for BNPF/HMTA resin across various heating rates.

phenol-formaldehyde (BNPF/HMTA) resins using non-isothermal differential scanning calorimetry (DSC) techniques. The results indicate that the incorporation of bio-oil as a partial substitute for phenol in the BNPF/HMTA formulation significantly reduced the curing temperature by approximately 20°C relative to the conventional NPF/HMTA resin system. This reduction in curing temperature is attributed to the chemical composition of bio-oil, which introduces additional reactive sites and modifies the crosslinking density within the resin matrix, facilitating earlier onset of crosslinking reactions and lowering the activation energy required for curing. As a result, the curing process is expedited, offering considerable advantages in energy efficiency, operational

Citation: Archana Bansode, Iris Beatriz Vega Erramuspe, Lorena Alexandra Portilla Villarreal, Braden Hahn, Brian K. Via, Allan David, Nicole Labbé, Maria L Auad. Reducing Activation Energy in Novolac Resins through Bio-Oil Integration: A Sustainable Approach. Journal of Radiology and Clinical Imaging 8 (2025): 88-99.

safety, and environmental sustainability by decreasing dependence on petroleum-derived phenol. The autocatalytic model showed strong alignment with the curing behavior of NPF/HMTA resin, while the Kamal model was most effective in characterizing the curing dynamics of BNPF/HMTA resin, where an autocatalytic mechanism dominated the initial phase, transitioning to an nth-order kinetic mechanism in later stages. These findings provide critical insights for the development and application of BNPF resins, particularly in contexts where lower curing temperatures and sustainability are paramount.

Acknowledgments:

References

1. Yan N, Zhang B, Zhao Y, et al., Application of Biobased Phenol Formaldehyde Novolac Resin Derived from Beetle Infested Lodgepole Pine Barks for Thermal Molding of Wood Composites. Ind Eng Chem Res 56 (2017): 6369–6377.

2. Berdnikova PV, Zhizhina, EG, Pai ZP. Phenol-Formaldehyde Resins: Properties, Fields of Application, and Methods of Synthesis. Catal Ind 13 (2021): 119–124.

3. Milazzo M, Amoresano A, Pasquino, R.; Grizzuti, N.; Auriemma, F.; De Stefano, F.; Sin Xicola, A.; Iodice, V.; De Rosa, C. Curing Efficiency of Novolac-Type Phenol–Formaldehyde Resins from Viscoelastic Properties. Macromolecules 54 (2021): 11372–11383.

4. Zhang X, Solomon DH. Chemistry of Novolac/Furfuryl Alcohol Resins Cured with Hexamethylenetetramine: A Solid-State NMR Study. Chemistry of Materials 10 (1998): 1833–1840.

5. De Medeiros ES, Agnelli JAM, Joseph K, et al., Curing Behavior of a Novolac-Type Phenolic Resin Analyzed by Differential Scanning Calorimetry. J Appl Polym Sci 90 (2003): 1678–1682.

6. Mahajan JS, O'Dea RM, Norris JB, et al., Aromatics from Lignocellulosic Biomass: A Platform for High-Performance Thermosets. ACS Sustain Chem Eng 8 (2020): 15072–15096.

7. Nolan Wilson A, Price MJ, Mukarakate C, et al., Integrated Biorefining: Coproduction of Renewable Resol Biopolymer for Aqueous Stream Valorization. ACS Sustain Chem Eng 5 (2017); 6615–6625.

8. Bansode A, Barde M, Asafu-adjaye O, et al., Synthesis of Biobased Novolac Phenol − Formaldehyde Wood Adhesives from Biore Fi Nery-Derived Lignocellulosic Biomass. ACS Sustain Chem Eng (2021).

9. Asafu-Adjaye OA, Street J, Bansode A, et al., Fast Pyrolysis Bio-Oil-Based Epoxy as an Adhesive in Oriented Strand Board Production. Polymers (Basel) 14 (2022): 1244.

10. Gupta N, Mahendran AR, Weiss S, et al., Thermal Curing Behavior of Phenol Formaldehyde Resin-Impregnated Paper Evaluated Using DSC and Dielectric Analysis. J Therm Anal Calorim 149 (2024): 2609–2618.

11. Chen Y, Fan D, Qin T, et al., Thermodegradation of PF Resin 9 (2014).

12. Zhao Y, Yan N, Feng M. Synthesis and Characterization of Bio-Based Phenol-Formaldehyde Resol Resins from Bark Autoclave Extractives. For Prod J 66 (2016): 18–28.

13. Li H, Wang S, Zhang X, et al., Synthesis and Characterization of an Environmentally Friendly Phenol–Formaldehyde Resin Modified with Waste Plant Protein. Polymers (Basel) 15 (2023).

14. Wuzella G, Mahendran AR, Beuc C, et al., Isoconversional Cure Kinetics of a Novel Thermosetting Resin Based on Linseed Oil. J Therm Anal Calorim 142 (2020): 1055–1071.

15. Zolghadr M, Zohuriaan-Mehr MJ, Shakeri A, et al.,. Epoxy Resin Modification by Reactive Bio-Based Furan Derivatives: Curing Kinetics and Mechanical Properties. Thermochim Acta 673 (2019): 147–157.

16. Ferdosian F, Zhang Y, Yuan Z, et al., Curing Kinetics and Mechanical Properties of Bio-Based Epoxy Composites Comprising Lignin-Based Epoxy Resins. Eur Polym J 82 (2016): 153–165.

17. Siddiqui H, Mahmood N, Yuan Z, et al., Sustainable Bio-Based Phenol-Formaldehyde Resoles Using Hydrolytically Depolymerized Kraft Lignin. Molecules 22 (2017).

18. Cui Y, Hou X, Wang W, et al., Synthesis and Characterization of Bio-Oil Phenol Formaldehyde Resin Used to Fabricate Phenolic Based Materials. Materials 10 (2017).

19. Song Y, Wang Z, Zhang X, et al., Synthetic Process of Bio-Based Phenol Formaldehyde Adhesive Derived from Demethylated Wheat Straw Alkali Lignin and Its Curing Behavior. J Renew Mater 9 (2021): 943–957.

20. Zhang C, Binienda WK, Zeng L, et al., Kinetic Study of the Novolac Resin Curing Process Using Model Fitting and Model-Free Methods. Thermochim Acta 523 (2011): 63–69.

21. Kim P, Weaver S, Noh K, et al., Characteristics of Bio-Oils

Citation: Archana Bansode, Iris Beatriz Vega Erramuspe, Lorena Alexandra Portilla Villarreal, Braden Hahn, Brian K. Via, Allan David, Nicole Labbé, Maria L Auad. Reducing Activation Energy in Novolac Resins through Bio-Oil Integration: A Sustainable Approach. Journal of Radiology and Clinical Imaging 8 (2025): 88-99.

Produced by an Intermediate Semipilot Scale Pyrolysis Auger Reactor Equipped with Multistage Condensers. Energy and Fuels 28 (2014): 6966–6973.

22. Thomas R. Sinturel C, Pionteck J. et al., In-Situ Cure and Cure Kinetic Analysis of a Liquid Rubber Modified Epoxy Resin. Ind Eng Chem Res 51 (2012): 12178–12191.

23. Patel A. Maiorana A, Yue L, et al., Curing Kinetics of Biobased Epoxies for Tailored Applications. Macromolecules 49 (2016): 5315–5324.

24. Perejón A, Sánchez-Jiménez PE, Criado JM, et al., Kinetic Analysis of Complex Solid-State Reactions. A New Deconvolution Procedure. Journal of Physical Chemistry B 115 (2011): 1780–1791.

25. Yang G, Yuan Z, Yang Z, et al., Nonisothermal Curing Kinetics of a Novel Polymer Containing Phenylsilylene and Propargyl-Hexafluorobisphenol a Units. J Appl Polym Sci 127 (2013): 3178–3185.

26. Wan J, Li C, Fan H, et al., Branched 1,6-Diaminohexane-Derived Aliphatic Polyamine as Curing Agent for Epoxy: Isothermal Cure, Network Structure, and Mechanical Properties. Ind Eng Chem Res 56 (2017): 4938–4948.

27. Mashouf Roudsari G, Mohanty AK, Misra M. Study of the Curing Kinetics of Epoxy Resins with Biobased Hardener and Epoxidized Soybean Oil. ACS Sustain Chem Eng 2 (2014): 2111–2116.

28. Li J, Qiao Y, Zong P, et al., Thermogravimetric Analysis and Isoconversional Kinetic Study of Biomass Pyrolysis Derived from Land, Coastal Zone, and Marine. Energy and Fuels 33 (2019): 3299–3310.

29. Friedman HL. Kinetics of Thermal Degradation of Char-Forming Plastics from Thermogravimetry. Application to a Phenolic Plastic. Journal of Polymer Science Part C: Polymer Symposia 6 (2007): 183–195.

30. Hao H, Chang T, Cui L, et al., Theoretical Study on the Mechanism of Hydrogen Donation and Transfer for Hydrogen-Donor Solvents during Direct Coal Liquefaction. Catalysts 8 (2018).

31. Langtry BN. Identity And Spatio-Temporal Continuity. Australas J Philos 50 (1972): 184–189.

32. Blaine RL, Kissinger HE. Homer Kissinger and the Kissinger Equation. Thermochim Acta 540 (2012): 1–6.

33. Vyazovkin S. Evaluation of Activation Energy of Thermally Stimulated Solid-State Reactions under Arbitrary Variation of Temperature. J Comput Chem 18 (1997): 393–402.

34. Hosseinpour A, Nazockdast H, Behzad T, et al., Investigation of the Cure Kinetics of an Epoxy Resin by Advanced Isoconversional and Model-Fitting Methods. AIP Conference Proceedings (2016).

35. Li S, Järvelä P. Application of a Model-Free Isoconversional Method to the Cure of Phenolic Systems. J Polym Sci B Polym Phys 39 (2001): 1525–1528.

36. Ma S, Fan H, Zhang N, et al., Investigation of a Low-Toxicity Energetic Binder for a Solid Propellant: Curing, Microstructures, and Performance. ACS Omega. (2020): 30538–30548.

37. Mashouf Roudsari G, Mohanty AK, Misra M. Study of the Curing Kinetics of Epoxy Resins with Biobased Hardener and Epoxidized Soybean Oil. ACS Sustain Chem Eng 2 (2014): 2111–2116.

38. Zhan X, Liu H, Zhang J. Two Branched Silicone Resins with Different Reactive Groups: A Comparative Evaluation. Ind Eng Chem Res 57 (2018): 5606–5615.

39. Zhou Z, Si Q, Wan L, et al., Curing Kinetics of Main-Chain Benzoxazine Polymers Synthesized in Continuous Flow. Ind Eng Chem Res 61 (2022): 2947–2954.

40. Horadam W, Venkat N, Tran T, et al., Leaching Studies on Novolac Resin-Coated Proppants-Performance, Stability, Product Safety, and Environmental Health Considerations. J Appl Polym Sci 135 (2018).

41. Domínguez JC, Alonso MV, Oliet M, et al., Kinetic Study of a Phenolic-Novolac Resin Curing Process by Rheological and DSC Analysis. Thermochim Acta 498 (2010), 39–44.
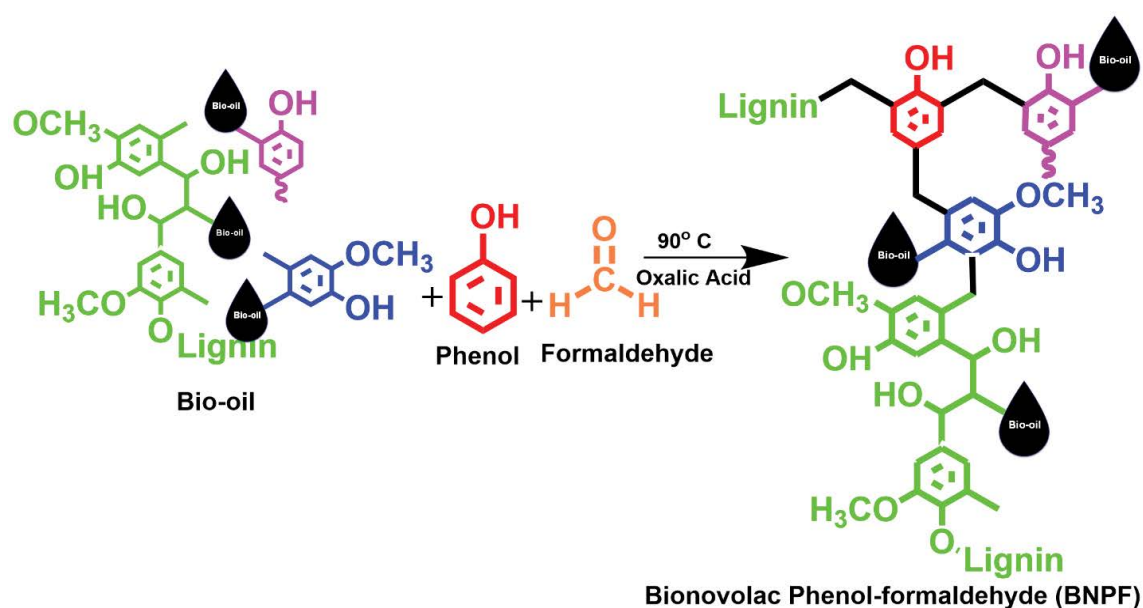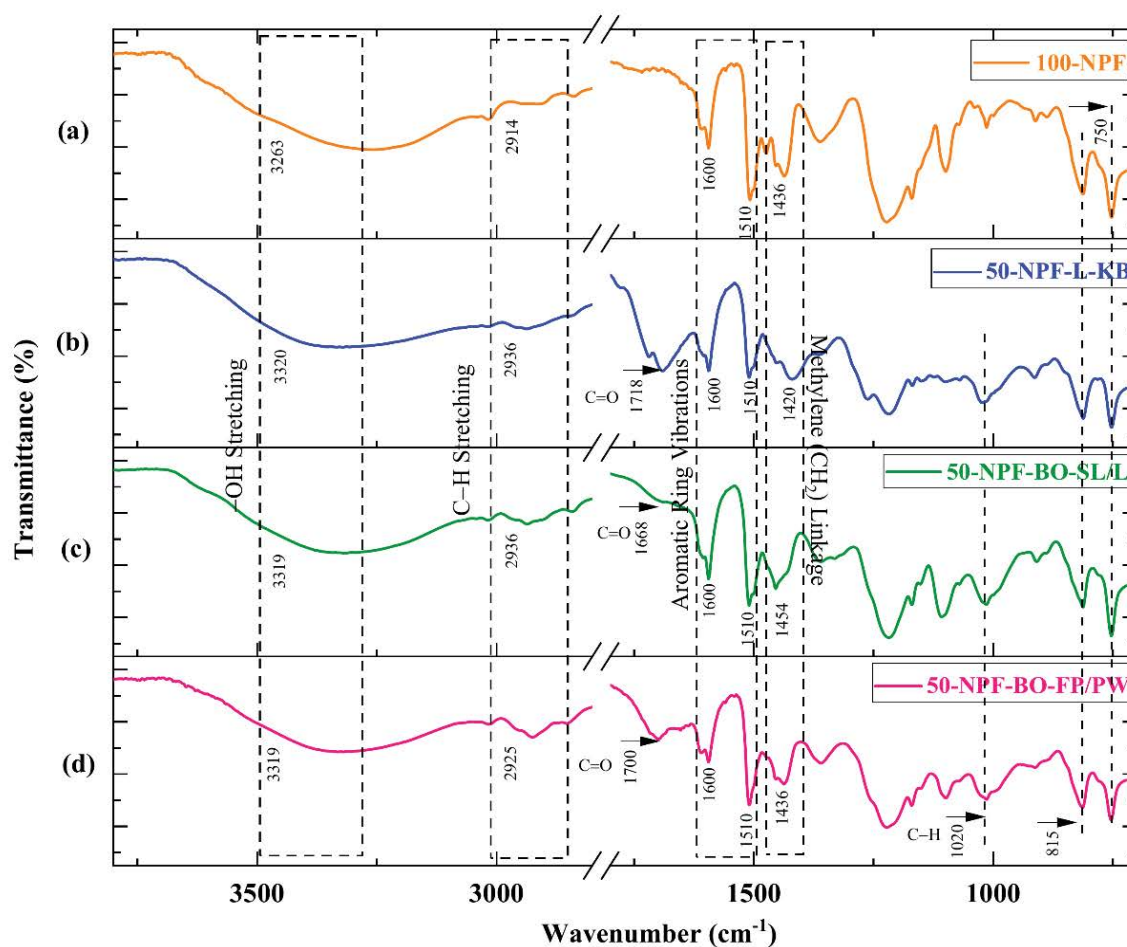
Figures S1: The reaction mechanism of bionovolac phenol-formaldehyde resin (BNPF)
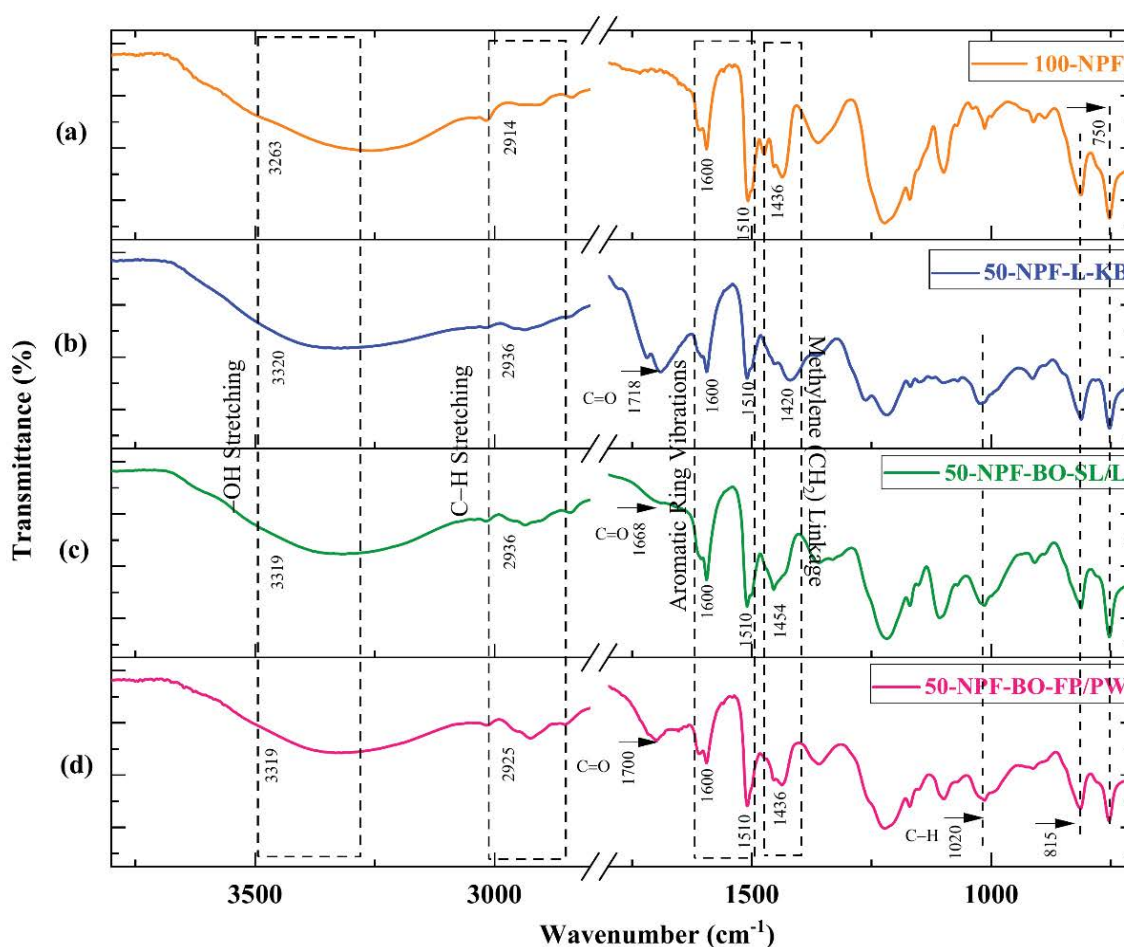
Figure S2 Resin characterization by FTIR (a) Novolac phenol-formaldehyde resin and, (d) biobased novolac phenol-formaldehyde resin [Adapted from our previous publication: Synthesis of Biobased Novolac Phenol–Formaldehyde Wood Adhesives from Biorefinery-Derived Lignocellulosic Biomass (2021) ACS Sustainable Chemistry & Engineering, 9 (33), 10990–11002.]

Citation: Archana Bansode, Iris Beatriz Vega Erramuspe, Lorena Alexandra Portilla Villarreal, Braden Hahn, Brian K. Via, Allan David, Nicole Labbé, Maria L Auad. Reducing Activation Energy in Novolac Resins through Bio-Oil Integration: A Sustainable Approach. Journal of Radiology and Clinical Imaging 8 (2025): 88-99.

Figure S3 Resin characterization by ^{1}H NMR (a) Novolac phenol-formaldehyde resin and, (d) bionovolac phenol-formaldehyde resin [Adapted from our previous publication: Synthesis of Biobased Novolac Phenol–Formaldehyde Wood Adhesives from Biorefinery-Derived Lignocellulosic Biomass (2021) ACS Sustainable Chemistry & Engineering, 9 (33), 10990–11002.]